CO-Induced Photoemission Structures of the CO/Pt/Ru(0001) Interface

P.J. Godowski[a,*], J. Onsgaard[b] and Z.-S. Li[c]

[a]Institute of Experimental Physics, University of Wrocław, Pl. M. Borna 9, 50-204 Wrocław, Poland
[b]Department of Physics and Nanotechnology, Aalborg University, DK–9220 Aalborg East, Denmark
[c]Institute of Storage Ring Facilities, University of Aarhus, DK–8000 Aarhus, Denmark

(Received May 12, 2016; in final form November 24, 2016)

The CO/Pt/Ru(0001) interface has been re-examined, in great detail, by photoelectron spectroscopy of high resolution under UHV conditions. The Ru(0001) substrate has been modified by platinum at coverages less than corresponding to the one, saturated, Pt overlayer, with no Pt/Ru intermixing. The analysis of the extent to which different regions of the photoelectron spectrum allow a detailed characterization of the interface is presented. The CO adsorption displays interaction with two separate phases: the Pt(111) face and the Ru(0001) surface.

DOI: 10.12693/APhysPolA.130.1389
PACS/topics: 79.60.Jv, 33.60.+q, 82.80.Pv

1. Introduction

In order to understand the phenomena occurring on the surface (adsorption, surface and bulk diffusion, atoms intermixing, surface reactions, etc.) in terms of their description and predictability, investigations of the solid surfaces are required. Metallic surfaces play a special role in the science, because the control of the phenomena taking place e.g. in heterogeneous catalysis, corrosion of metals and their alloys as well as predicting the adhesion properties of metals are essential in modern material science. It is worth noting that the surface science is a precursor of nanotechnology in the field of proper shaping of structures and properties of the surface layers of metals. The study of the interaction of carbon monoxide with transition metal surfaces has been of interest for technological application (catalysis) and for the theoretical point of view. In the past few decades, various surface science techniques and theoretical methods have been employed to this, so-called, model adsorbate system. By establishing a correlation between spectroscopic data and the chemisorption energy (e.g. CO on a series of metal surfaces [1]) it is possible to predict the surface chemical activity based on the electronic properties only.

It is known that on the Ru(0001) surface at temperatures less than 520 K, under vacuum conditions CO adsorbs non-dissociatively in the upright position with the C end facing the surface. Consequently, adsorbed CO forms a number of ordered phases, namely $(\sqrt{3} \times \sqrt{3})R30°$ at a coverage of 0.33 SML (substrate monolayers, i.e. coverage expressed relative to the number of the surface atoms) [2]; and two low temperature coverages (existing at $T < 200$ K) exceeding 1/3: $(2\sqrt{3} \times 2\sqrt{3})R30°$ at 0.58 SML; $(5\sqrt{3} \times 5\sqrt{3})R30°$ at 0.65 SML [3, 4]. Experiments performed at elevated pressures (up to 1 Torr) showed similar results except that carbon builds-up on the surface at lower temperatures, i.e. at 300 K due to CO dissociation [5].

Platinum deposited on Ru(0001) at room temperature (RT) in submonolayer amount forms small, homogeneously distributed, two-dimensional islands with a relaxed, dendritic shape [6, 7]. The condensate structure is compatible with the Pt(111) face and contains a big fraction of edge sites. At 870 K, the transformation from a relaxed to stressed (polymorphic) phase was detected from the Pt $4f$ binding energy (BE) shift. Up to *ca.* 970 K any Pt/Ru intermixing is not expected [7, 8].

On the Pt(111) surface carbon monoxide adsorbs molecularly, with a comparable bond to that on ruthenium and the perpendicular orientation [9]. The saturated layer is a mixture of on-top and bridge sites with a 1:1 ratio [10, 11]. At 300 K, LEED shows the $c(4 \times 2)$ structure corresponding to the 0.50 SML at saturation with coexistence of two inequivalent sites [12]. At lower coverages, mostly on-top sites are filled.

Adsorption of low CO coverage on Pt layers on Ru(0001) has been studied using infrared-absorption spectroscopy, scanning tunnelling microscopy, and thermal desorption spectroscopy [13]. The results were discussed in context of thin film structural (lateral strain, defects) and electronic points of view.

In this paper, systematic investigations of CO adsorption on a platinum-modified ruthenium substrate, re-examined by photoemission of high resolution, are presented. The modification of the interface is simple, as it refers to the two separate phases, Ru and Pt, with minor influence of the subsurface ruthenium layer on the interaction with the adsorbed molecules.

2. Experimental

The experiments were performed at the ISA Centre for Storage Ring Facilities (ASTRID2, Aarhus, Denmark) using the AU-Matline end station. The material science beamline with the use of a multipole wiggler

*corresponding author; e-mail: pjg@ifd.uni.wroc.pl

served the photon energy in the range of 20–700 eV [14]. The ultra-high vacuum (UHV) chamber (base pressure of 6.0×10^{-8} Pa) was equipped with standard surface techniques for surface preparations and characterization. The UHV system contained a Scienta electron energy analyser and SX-700 monochromator.

The Ru(0001) sample was mounted on a heating device attached to a dewar giving the possibility of cooling to 115 K and heating (by e-bombardment) to 1300 K. The temperature of the sample was measured with a K-type thermocouple (chromel–alumel; $Ni_{90}Cr_{10}$–$Ni_{95}Mn_2Al_2Si_1$) spot-welded to the rear part.

The Ru(0001) single crystal was cleaned by repeated cycles of Ar^+ ion bombardment (1.0 keV, $p_{Ar} = (3-4) \times 10^{-3}$ Pa, 25 min) followed by flash annealing to 1300 K. Surface cleanliness was checked by the 5/2 to 3/2 intensity ratio of the $3d$ Ru band to that expected for clean ruthenium at given settings of the electron energy analyzer and accompanied software (the C $1s$ peak overlaps with the Ru $3d_{3/2}$ peak).

The Pt-modified ruthenium surfaces were prepared by vapor deposition of Pt (e-bombardment heating) on substrate at RT. At the end of longer time of evaporation, the pressure of residual gases increased to 8.0×10^{-7} Pa. After adsorption we have received in the first case $I(\theta)/I = 0.9737$ and 0.8220 for the second case and the Pt coverage has been evaluated (Appendix) as 0.06 and 0.42 monolayer, respectively. Hence, the rate of deposition is equal to 4.5×10^{-4} monolayers per second, ML/s. For the two coverages under investigations, 0.06 and 0.42 adsorbate monolayer (AML), we expect small and larger Pt islands of ramified shape on the substrate, respectively, with the platinum lattice constant of (111) orientation.

CO was admitted to the whole chamber via a dosing system. A typical dose of 1.0 L corresponded to 2 s of 6.67×10^{-5} Pa (5.0×10^{-7} Tr). The saturation layer of CO was achieved after 5 to 15 L.

The spectra of the regions were normalized taking the average intensity of the last 10 points of the high kinetic energy side (where the background hardly changes) as equal to the 1.00 level. In the case of the valence band (VB) spectra the 1.00 level was taken as the aligned average intensity (noise) corresponding to kinetic energies greater than the applied photon beam energy. For each region of the spectrum the appropriate part of the valence band containing the Fermi level was registered. The edge was determined using the step function $(a/(1 + \exp((x - b)/c))) + d$ where x denotes kinetic energy and a, b, c, d are parameters and the value obtained was used to determine the binding energy (BE) with high precision. In the present work, assigned uncertainty corresponds to the reproducibility of the spectrum.

3. Results and discussion

3.1. Ru(0001)

The sputter-cleaned Ru(0001) single crystal shows the Ru $3d$ doublet, Fig. 1, at 279.79(4) eV ($3d_{5/2}$) with a spin–orbit splitting (SOS) of 4.17 eV. Due to the Coster–Kronig effect, the full width at half maximum (FWHM) of the $3d_{3/2}$ is greater than the one of the $3d_{5/2}$. The fitting is achieved using an asymmetric line shape. For the instrument and the acquisition system measurements employed in this study, the parameters of the fitting procedure are determined as collected in Table I. The values presented are consistent with the literature.

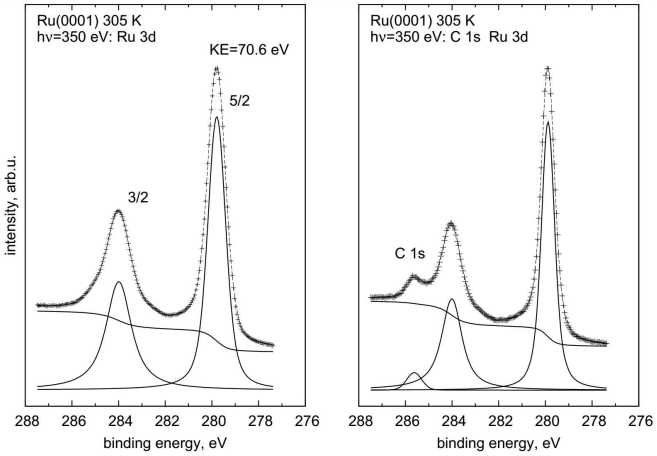

Fig. 1. Ru $3d$ region of spectra before (left part) and after exposure to 55 L of CO (right part) at 305 K. The experimental data are crosses, the solid lines are the background and individual peaks from fitting of the data.

TABLE I

Ru metal, $3d$. Binding energy, separation and FWHM are given in eV.

BE($3d_{5/2}$)	Doublet sep.	% Int. ratio	FWHM ratio	Ref.
280.0(1)	4.10–4.20			[15]
279.8(7)	4.17	60/40	0.48/0.92	[16]
279.79(4)	4.17	61/39	0.80/1.29	this work

3.2. Ru(0001)–CO

Typical spectra obtained from CO adsorbed on the ruthenium surface and the results of the spectra synthesis are shown in Fig. 2 and summarized in Table II. From the attenuation of the Ru $3d_{5/2}$ peak, ratio of intensities of 0.7283, the CO coverage of saturated layer was evaluated (Appendix) as equal to 0.96 of the full $(\sqrt{3} \times \sqrt{3})R30°$ structure. The left part of the figure shows the O $1s$ peak and the right part displays the VB. The results concerning the C $1s$ peak are shown in the right side of Fig. 1. In this case, i.e. adsorption at around RT, practically any complexity of the O $1s$ peak was not observed.

Normal emission VB spectra show a similarity between the adsorbate resonances and the gas phase spectrum of carbon monoxide. The similarity to the gas phase spectra supports the interpretation of CO as molecular (associative) with bonding to the metal surface through the carbon atom. Two prominent peaks are assigned to the 4σ and $5\sigma/1\pi$ orbitals of the free molecule based on comparison with the gas phase spectrum and the metal carbonyl

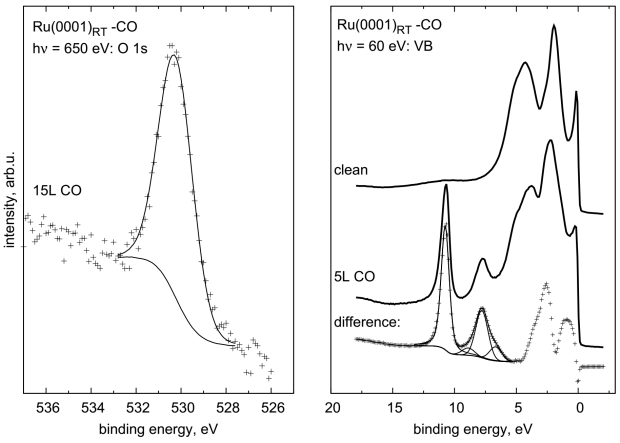

Fig. 2. O 1*s* region obtained after CO adsorption on Ru(0001) with peak synthesis (left part). VB region of spectra before and after exposure to 5 L of CO (right part) at room temperature (normal emission). The difference spectrum was useful in the analysis of the CO-derived orbitals.

TABLE II

VB and O 1*s* spectra of adsorbed CO at room temperature. BE, FWHM is given in eV. %ts denotes percent of total signal (area).

Interface	Peak	Position	FWHM	%ts
$Ru(0001)_{RT}$–CO	VB: satell.	6.68	1.16	8
	CO: $1\pi/5\sigma$	7.78	1.16	28
	VB: satell.	8.88	1.16	4
	CO: 4σ	10.75	0.78	60
	CO: C 1*s*	285.53	1.04	100
	CO: O 1*s*	530.23	1.77	100
annealed to 510 K	C 1*s*	282.52	0.60	19
$Ru(0001)_{115K}$–CO	CO: O 1*s*	530.52	1.68	85
	CO: O 1*s*	528.81	1.68	15

spectrum. The 4σ peak position shifts slightly (less than 0.1 eV) towards higher BE with coverage. These findings are consistent with those published by other authors [17].

It is interesting that the 4σ feature has no satellite on the high binding energy side as it was observed for the copper substrate. In the CO/Cu case, the 4σ satellite has an intensity near 36% of the main peak and the intensity ratio was indicative for the CO–substrate interaction [18, 19]. Consequently, the registered 1*s* spectra of carbon and oxygen do not contain satellites [20, 21] as it could be seen in Figs. 1 and 2 and due to that the synthesis of the spectra is greatly simplified.

The spectra registered with increasing temperature from RT are collected in Fig. 3. The peaks corresponding to adsorbed CO, i.e. the C 1*s* peak lying on the slope of the Ru 3*d*3/2, the CO 4σ and $1\pi/5\sigma$ molecular features of the VB and O 1*s* peak decrease in intensity and finally disappear at temperatures exceeding *ca.* 510 K. The oxygen-free ruthenium surface could only be obtained by annealing. In the Ru 3*d* region (not shown in Fig. 3), the peak at BE = 282.52 eV of small

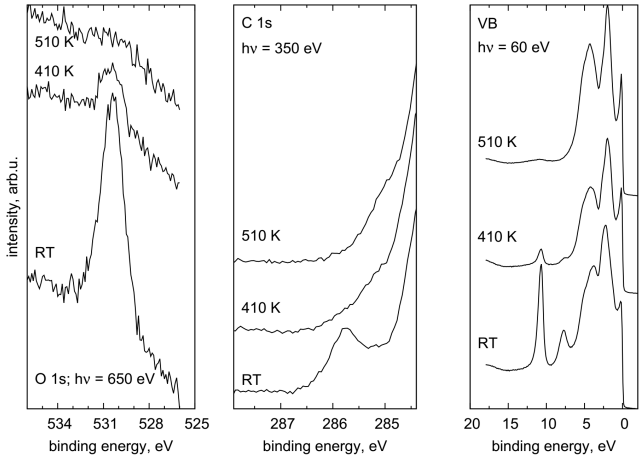

Fig. 3. The spectra (normal emission) before and after annealing the $Ru(0001)_{RT}$–CO interface to the indicated temperatures: O 1*s* region (left part), C 1*s* region (middle part) and VB region (right part).

intensity (Table II) left after desorption of carbon monoxide molecules. Due to the temperature involved in the annealing process, it is assigned to a carbidic form of the C 1*s* feature [22]. The presence of this, small intensity carbide peak, was confirmed by inspection of the difference spectra derived from a sample clean and after desorption. During annealing to 510 K, a small amount of CO molecules dissociate, probably at the surface defects, leaving the carbide on the surface.

The spectra corresponding to the low temperature (115 K) adsorption look similar except the O 1*s*. The VB spectrum contains the CO 4σ and $1\pi/5\sigma$ orbitals separated by a distance of 2.95–3.00 eV. The region of the O 1*s* shows an additional peak of low intensity located 1.71 eV lower than the BE of the peak attributed to CO adsorbed on-top. Due to low temperature adsorption, the coverage of CO at saturation is higher than before. Our calculation (Appendix) based on the Ru $3d_{5/2}$ intensity ratio of 0.6531 gives a value of 1.22 relative to the $(\sqrt{3}\times\sqrt{3})R30°$ structure, i.e. it is higher than 0.33 SML and consequently additional molecules of CO adsorb in bridge position, BE(on-top) > BE(bridge). The absolute values of the O 1*s* binding energies are 1.4–1.7 eV lower than those published by Starr and Bluhm [5].

3.3. $Ru(0001)_{RT}$–(0.06 AML)$Pt(111)_{115K}$–CO

The Pt 4*f* spectra obtained from a small amount of deposit (0.06 AML) at different stages of the experiment are displayed in Fig. 4 (left part). Typical spectrum of the interface after platinum deposition at RT contains two distinct features, at 71.06 and 74.37 eV (SOS = 3.31 eV), corresponding to the $4f_{7/2}$ and $4f_{5/2}$ emissions. The peaks are broadened due to the morphology of the adsorbate. At high BE side of both peaks, additional spectral weight is associated. The 4*f* Pt spectra do not show separate surface and bulk contributions of the signal because the expected energy shift is smaller than overall experimental resolution of the system.

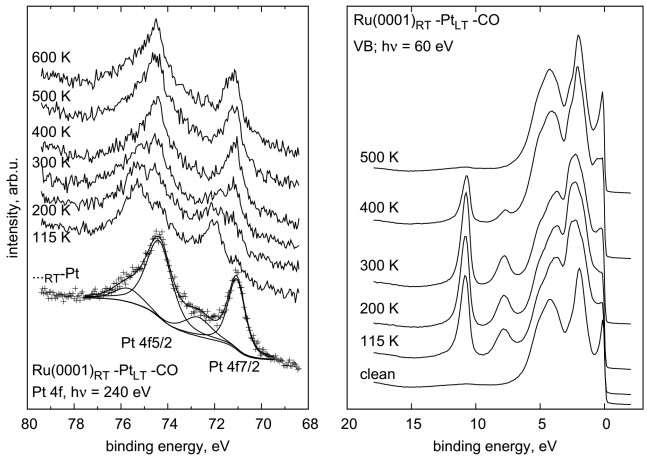

Fig. 4. Left part: Pt $4f$ spectra ($h\nu = 240$ eV; normal emission) with peak synthesis. Right part: VB spectra obtained during experiment ($h\nu = 60$ eV; normal emission) at the indicated temperatures.

After saturation of the modified interface with CO at 115 K, the CO-induced Pt $4f$ peaks show shift by $\approx$ 1.0 eV towards higher BE. Those lines dominate in the total spectrum. At 300 K, two CO-induced peaks are of smaller intensity which is a consequence of desorption of molecules, particularly those involved platinum. It seems that the desorption starts at lower temperatures than on the pure Ru(0001) or Pt(111) surfaces. The Pt $4f$ spectrum returns to the initial one after annealing the interface at 500 K. From the other hand, total CO desorption takes place at the same temperature as that observed for pure substrate. For such adsorbate behavior, adsorption close to the Pt island edges could be responsible.

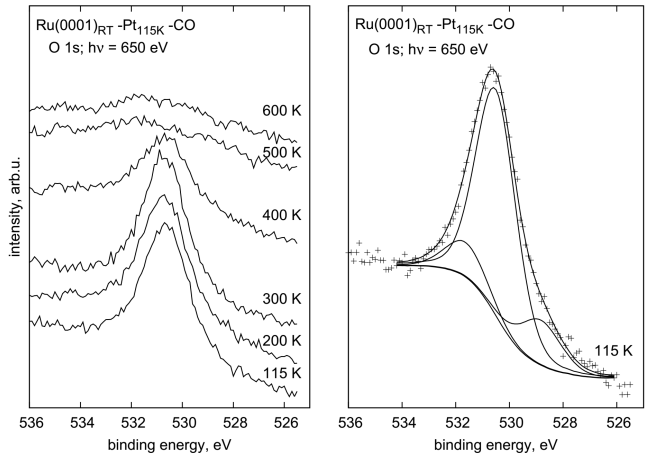

Fig. 5. O 1s spectra obtained during experiment ($h\nu = 650$ eV; normal emission) at indicated temperature. O 1s peak at 115 K is presented with peak synthesis.

The O 1s peaks corresponding to low temperature adsorption of CO on the Ru(0001)–Pt interface are collected in Fig. 5. The fine structure of the peak indicates the possibility of the contribution of three components. This is confirmed by analysis of the 1s feature obtained at high temperature. Three contributions indicate that molecular CO adsorb additionally on sites other than on-top Ru. The bridge bonded CO on Ru is represented by peak at lower BE than the main oxygen peak (Table III). Third peak in the O 1s spectrum with a binding energy of 531.63 eV is interpreted as coming from adsorbate on platinum. The intensity, expressed by the percent of total signal (%ts), is proportional to the amount of adsorbate, respectively.

TABLE III

O 1s spectra of adsorbed CO at 115 K on Pt covered Ru(0001) of 0.06 AML. BE, FWHM is given in eV. %ts denotes percent of total signal (area).

Interface	Peak	Position	FWHM	%ts
$Ru(0001)_{RT}$–Pt_{115K}-CO	CO: O 1s	528.83	1.80	14
	CO: O 1s	530.50	1.76	74
	CO: O 1s	531.63	1.80	12
annealed to 400 K	CO: O 1s	528.67	1.77	20
	CO: O 1s	530.46	1.77	67
	CO: O 1s	531.61	1.77	13

3.4. $Ru(0001)_{RT}$–(0.42 AML)$Pt(111)_{RT}$–CO

Series of spectra corresponding to the Pt(0.42 AML)-modified ruthenium interface, the O 1s, valence band and the Pt $4f$ are collected in Fig. 6 and Fig. 7, respectively. Room temperature adsorption of CO at higher coverage of platinum shows qualitatively similar results to the previous ones. Due to the adsorption at room temperature and as a consequence of a smaller saturation coverage of CO, the O 1s additional contributions exhibit relative lower intensities (Table IV). Similarly, the CO-induced Pt peaks are visible as a shoulder on the high binding energy side of the main peak.

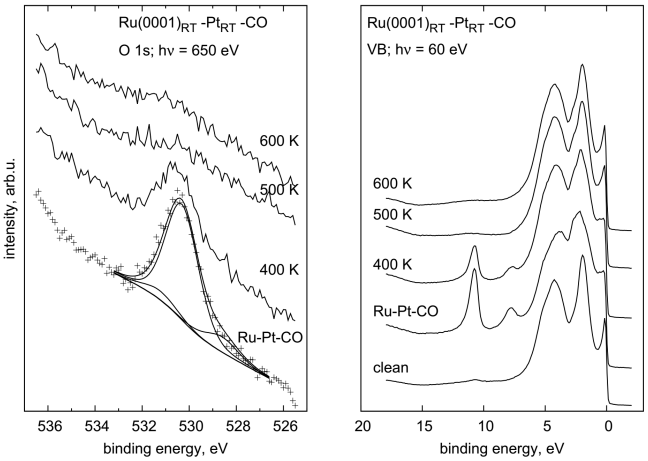

Fig. 6. Left part: O 1s spectra ($h\nu = 650$ eV; normal emission); the peak synthesis shows the contribution of three components. Right part: VB spectra obtained during experiment ($h\nu = 60$ eV; normal emission) at the indicated temperatures.

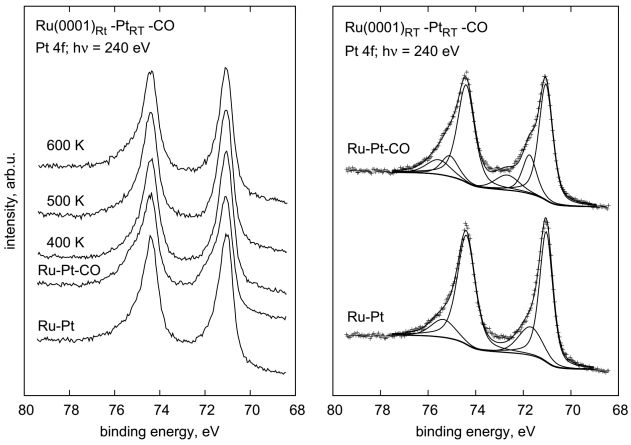

Fig. 7. Left part: Pt $4f$ spectra obtained during experiment ($h\nu = 240$ eV; normal emission) at the indicated temperatures. Right part: the Pt $4f$ peak synthesis for identification of the CO-induced Pt contribution.

TABLE III

O $1s$ spectra of adsorbed CO at RT on Ru(0001) with Pt coverage of 0.42 AML. BE, FWHM is given in eV. %ts denotes percent of the total signal (area).

Interface	Peak	Position	FWHM	%ts
$Ru(0001)_{RT}$–Pt_{RT}–CO	CO: O 1s	528.48	1.70	14
	CO: O $1s$	530.31	1.70	78
	CO: O $1s$	531.60	1.70	8
annealed to 400 K	CO: O $1s$	528.52	1.63	17
	CO: O $1s$	530.36	1.63	72
	CO: O $1s$	531.25	1.63	11

4. Conclusions

The interaction of CO with the Pt-modified Ru(0001) surface was studied by means of photoelectron spectroscopy using synchrotron radiation. Carbon monoxide was adsorbed at low (115 K) and at room temperature. The C $1s$ peak, overlapping the region of the Ru $3d_{3/2}$ peak, corresponding to the molecular adsorption is clearly distinguished and desorbs under temperature treatment. Chemisorbed CO shifts the Pt $4f$ peaks by ≈ 1.0 eV towards higher BE which is quite prominent at very low platinum coverages. The Pt islands influence as well the range of desorption temperatures of the adsorbed molecules. In addition to the peak representing "on-top" molecular geometry, the O $1s$ feature of the modified interfaces shows an additional contribution which is identified as "bridge-bonded" CO. In the valence band, the 4σ and $5\sigma/1\pi$ orbitals are unaffected by the adjacent platinum atoms.

Appendix: Evaluation of adsorbate coverage

Up to one monolayer, the photoemission signal changes linearly with coverage [23] and for the substrate we have

$$I(\theta) = I - [I - I(1)]\theta,$$

where I denotes the intensity of the photoelectron transition of the substrate without the adsorbate, θ is the coverage ($0 \le \theta \le 1$) and $I(1)$ denotes the signal corresponding to the substrate covered with the one adsorbate layer, i.e. the surface saturated with adsorbate at given experimental conditions. Rearranging the above equation we obtain

$$\theta = \frac{I - I(\theta)}{I - I\exp(-1/\lambda)} = \frac{1 - I(\theta)/I}{1 - \exp(-1/\lambda)}.$$

Then, the surface coverage, θ, can be calculated on the basis of the substrate signal only on the condition of that the electron escape depth, λ (in monolayers), is known. The λ quantity could be evaluated with the help of the Seah–Dench formula [24]. Because the photoelectrons have been registered along the surface normal, the electron escape depth has the same value as the attenuation length.

Pt coverage

The platinum coverage was determined by taking into account the areas under the Ru $3d_{5/2}$ peak before and after adsorption. The practical monolayer thickness of platinum, calculated from the density of Pt, 21.45×10^3 kg/m^3, is equal to $\bar{a}_{\mathrm{Pt}} = 247.2$ pm. Using the formula for elements [24], $\lambda_{\mathrm{AL}} = 538\times10^{-2}+0.41(\bar{a}\times10)^{0.5}$, the AL of the 70.6 eV electrons through the Pt layer is equal to 1.82 practical monolayers (PML). The PML is approximation of the quantity in units of the AML.

CO coverage

The monolayer thickness of CO can be approximated in several ways. The distance between the planes of ruthenium and of oxygen, for the C≡O (molecular triple bond) adsorbed on-top, is equal to $\bar{a} = r(\mathrm{Ru,at.}) + 2r(\mathrm{C,molec.3b}) + r(\mathrm{O,molec.3b}) = 0.130 + 2 \times 0.060 + 0.053 = 0.303$ nm, where r denotes suitable radii [25]. The calculated density of the $(\sqrt{3} \times \sqrt{3})R30°$ structure with the above mentioned height slightly exceeds (*ca.* 3%) the density of CO in the liquid state. On the other hand, a calculation based on the density of liquid CO, 0.789×10^3 kg/m^3, results in $\bar{a}_{\mathrm{CO}} = 0.3089$ nm, which seems to be a good approximation for calculating the electron escape depth. Using the formula for inorganic compounds, namely oxides [24], $\lambda_{\mathrm{AL}} = 2170 \times 10^{-2}+0.55(\bar{a}\times10)^{0.5}$ PML, the attenuation length of the 70.6 eV photoelectrons through the adsorbate is equal to 3.00 PML or AML.

Acknowledgments

The research leading to these results has received funding from the European Community Seventh Framework Programme (FP7/2007-2013) under grant agreement no. 226716.

References

[1] J.A. Rodriguez, D.W. Goodman, *Science* **257**, 897 (1992).

[2] P. Jakob, *J. Chem. Phys.* **120**, 9286 (2004).

[3] J.A. Herron, S. Tonelli, M. Mavrikakis, *Surf. Sci.* **614**, 64 (2013).

[4] Q. Chen, J. Liu, X. Zhou, J. Shang, Y. Zhang, X. Shao, Y. Wang, J. Li, W. Chen, G. Xu, K. Wu, *J. Phys. Chem. C* **119**, 8626 (2015).

[5] D.E. Starr, H. Bluhm, *Surf. Sci.* **608**, 241 (2013).

[6] P.J. Godowski, Z.-S. Li, J. Bork, J. Onsgaard, *Surf. Rev. Lett.* **14**, 911 (2007).

[7] P.J. Godowski, J. Onsgaard, Z. Ryszka, Ł. Rok, Z.-S. Li, *Surf. Sci.* **602**, 465 (2008).

[8] F. Buatier de Mongeot, M. Scherer, B. Gleich, E. Kopatzki, R.J. Behm, *Surf. Sci.* **411**, 249 (1998).

[9] P.R. Norton, J.W. Goodale, E.B. Selkirk, *Surf. Sci.* **83**, 189 (1979).

[10] R.C. Baetzold, G. Apai, E. Shustorovich, R. Jaeger, *Phys. Rev. B* **26**, 4022 (1982).

[11] M. Kinne, T. Fuhrmann, C.M. Whelan, J.F. Zhu, J. Pantförder, M. Probst, G. Held, R. Denecke, H.P. Steinruck, *J. Chem. Phys.* **117**, 10852 (2002).

[12] F. Bondino, G. Comelli, F. Esch, A. Locatelli, A. Baraldi, S. Lizzit, G. Paolucci, R. Rosei, *Surf. Sci.* **459**, L467 (2000).

[13] P. Jakob, A. Schlapka, *Surf. Sci.* **601**, 3556 (2007).

[14] www.isa.au.dk.

[15] A.V. Naumkin, A. Kraut-Vass, S.W. Gaarenstroom, C.J. Powell, in: *NIST X-ray Photoelectron Spectroscopy Database*, Version 4.1, Gaithersburg 2012.

[16] D.J. Morgan, *Surf. Interface Anal.* **47**, 1072 (2015).

[17] T. Pelzer, M. Grüne, K. Wandelt, *Progr. Surf. Sci.* **74**, 57 (2003).

[18] S.V. Christensen, J. Nerlov, P.J. Godowski, J. Onsgaard, *J. Chem. Phys.* **104**, 9613 (1996).

[19] P.J. Godowski, J. Onsgaard, S.V. Christiansen, J. Nerlov, *Acta Phys. Pol. A* **89**, 657 (1996).

[20] P.J. Godowski, A. Groso, S.V. Hoffmann, J. Onsgaard, *Acta Phys. Pol. A* **117**, 928 (2010).

[21] P.J. Godowski, S.V. Hoffmann, J. Onsgaard, *J. Electron. Spectrosc. Relat. Phenom.* **182**, 127 (2010).

[22] D.W. Goodman, J.M. White, *Surf. Sci.* **90**, 201 (1979).

[23] P.J. Godowski, *Acta Phys. Pol. A* **85**, 843 (1994).

[24] M.P. Seah, in: *Practical Surface Analysis*, 2nd ed., Vol. 1, Eds. D. Briggs, M.P. Seah, Wiley, 1990, Ch. 5.

[25] www.webelements.com.